Iranian Journal of Electrical and Electronic Engineering 01 (2020) 74–84
Special Issue on Electrical Machines and Drives

IUST
Iran University of Science and Technology

Iranian Journal of Electrical and Electronic Engineering

Journal Homepage: ijeee.iust.ac.ir

Research Paper

Improvement of Electromagnetic Forces in a Single-Phase Induction Motor by Providing a New Winding Distribution

H. Shadfar* and H. R. Izadfar*(C.A.)

Abstract: Single-phase induction motors have a wide range of domestic and industrial applications. These motors have a squirrel cage rotor and their stator usually has two windings: main and auxiliary. The use of auxiliary winding in the structure of single-phase induction motors creates two unbalance and asymmetric phases. This causes to increase the spatial harmonics of the field in the air gap, and also useless electromagnetic forces. The purpose of this paper is the reduction of the electromagnetic forces in single-phase induction motors, focusing on the effect of the stator winding distribution. For this purpose, two new and different winding distributions for the motors used in the water coolers will be provided. The produced electromagnetic forces in several conventional single-phase induction motors will be compared with new and conventional windings by means of numerical methods. Numerical analysis is performed by Maxwell software. The results of this analysis indicate improvements in the quality of the performance of these motors in the presence of the provided windings.

Keywords: Auxiliary Winding, Electromagnetic Noise, Main Winding, Single-Phase Induction Motor, Squirrel Cage Rotor, Starting Torque.

1 Introduction

SINGLE-PHASE induction motors are widely used in domestic, commercial and small workshops. In this motor, the stator has main and auxiliary windings, which their magnetic axis has some phase difference toward each other. The rotor of this motor is a squirrel cage [1].

One of the important issues in the process of designing electric machines is the problem of magnetic forces and the resulting vibration. When a device has abnormal vibration and noise, it must be quickly detected and also resolved or modified. Noises in electric machines are divided into four categories of mechanical, aerodynamic, electronic and electromagnetic [2].

The mechanical noise is produced by bearing defects, sliding contacts, shaft bending, couplings, U-shaped contacts, gears, and so on. The aerodynamic noise often occurs around the cooling system of the machine or parts that behave like a fan in the vicinity of the machine [3]. Electronic noises occur on most electric machines that have a drive system. In them, the supplied voltage contains many harmonics. Sometimes the forces at these frequencies are large enough and cause considerable noise, especially if they have values close to natural stator frequencies. Electromagnetic noises are usually produced by interactions of flux waves and resonant frequencies of the stator core or teeth. The magnetic field in the air gap is not monotonous and consists of variable harmonics due to various factors that can generate noise and vibration [4].

Extensive researches have been conducted to understand the nature and mechanism of the production of electromagnetic noise in squirrel cage induction motors. The resonance frequencies and the vibration of the stator of electric machines in different sizes are determined in [5, 6]. Calculation and analysis of electromagnetic noise are done by analytical methods in [7-10]. The calculation of the noise and vibration by numerical methods is also of interest to many researchers [11-13]. The evaluation of magnetic noise

Iranian Journal of Electrical and Electronic Engineering, 2020.
Paper first received 02 May 2019, revised 09 November 2019, and accepted 16 November 2019.
* The authors are with the Faculty of Electrical and Computer Engineering, Semnan University, Semnan, Iran.
E-mails: h.shadfar@semnan.ac.ir and hrizadfar@semnan.ac.ir.
Corresponding Author: H. R. Izadfar.

can be effective and useful in acoustic noise studies of electric machines [14-16]. One of the suitable methods for evaluating the electromagnetic noise is the calculation of the machine's natural frequencies [6, 17]. Magnetic noise reduction methods have also been studied in many papers such as [8, 9], [18-21]. The effect of various parameters, such as saturation [8], number of slots [10, 15], rotor eccentricity [22], on the magnetic noise is taken into consideration by some researchers. In addition to the expressed parameters, the phenomenon of the magnetostriction and the magnetic noise also interact. Generally, the electromagnetic forces in the air gap are divided into two groups: magnetostriction and Maxwell forces. Often the magnetostriction impacts low frequencies, particularly components with a frequency of twice the fundamental frequency [23-25]. Maxwell forces concentrate in the air gap related to the stator and the rotor, while the magnetostriction forces are applied into the stator and rotor steel sheet. Therefore, most of the papers ignore these forces and focus mainly on the noise generated by Maxwell forces. Maxwell forces are divided into two categories: radial and tangential. In induction machines, radial forces are dominant and tend to bring stator and rotor closer to each other [26]. Reducing harmonics in the air gap plays an important role in reducing electromagnetic noise. This purpose, can be done by some strategies such as: appropriate design of the geometry of the stator and rotor slots [15], the proper selection of the stator and rotor slots [10], the use of skewed slots in the rotor [27], the increase of air gap [28, 29], the correct selection of the suitable capacitor [30] and the proper winding distribution [31, 32]. In [31], a reference current that equals one-fourth of the main winding current is injected into the auxiliary winding of the single-phase induction motor. In [30], by maintaining the positive component of the current, the negative component is weakened around the rated load. For this purpose, non-orthogonal armature windings are used. In [32], reduces the electromagnetic noise and vibration in the single-phase induction machines by weakening the negative current component.

The purpose of this paper is to reduce electromagnetic forces in single-phase induction motors by choosing the appropriate pitch and distributing the windings. This will reduce the magnetic noise in these electric machines. The main focus of this is on two-speed induction motors used in water coolers. The main specifications of these motors are 0.75hp (at high speed i.e. 4-poles operation), 0.25hp (at low speed, i.e.6-poles operation), 220V, and 50Hz. The reason for choosing this motor is its vast production and application. This motor is currently available in both the Westinghouse American designs and the Italian design on the market. In this paper, the effect of the winding of these two designs on the distribution of magnetic fields and electromagnetic forces is evaluated. Then, two new winding distributions will be presented for these motors. A comprehensive comparison will be made between the existing and proposed windings. This comparison is based on analytical relationships as well as numerical simulations. The results of the studies indicate the improved motor performance and reduced magnetic noise of the machine in the presence of proposed windings. This study is conducted under the following assumptions.

- The induction machine is completely healthy and is supplied by an absolutely sinusoidal voltage, without any harmonic.
- The saturation of cores is ignored.

The rest of the paper is constructed as follows. In Section 2, the calculation of electromagnetic pressure is provided. Section 3 depicts the common single-phase induction motors. In Section 4, we can see an introduction to the new winding designs to reduce magnetic pressure. In Section 5, an analysis and comparison of different windings are presented. Finally, the paper is concluded in Section 6.

2 Calculation of Electromagnetic Pressure

Maxwell's radial forces are the main source of stator vibration and electromagnetic noise. Maxwell's radial pressure is Maxwell's radial force per unit area (P_m). In the air gap, it can be calculated by (1) [33].

$$P_m(\theta,t)=\frac{b_r^2(\theta,t)-b_t^2(\theta,t)}{2\mu_0} \tag{1}$$

In the Eq. (1), θ is the mechanical angular position in degree, μ_0 is the magnetic permeability in the air gap and $b_r(\theta, t)$, $b_t(\theta, t)$ are the radial the tangential components of flux density in the air gap, respectively. When $b_t(\theta, t)$ is much smaller than $b_r(\theta, t)$, it can be ignored in the analysis. Therefore, Eq. (1) can be simplified as (2).

$$P_m(\theta,t)=\frac{b_r^2(\theta,t)}{2\mu_0} \tag{2}$$

where, $b_r(\theta, t)$ is defined as (3).

$$b_r(\theta,t)=f(\theta,t)\lambda(\theta,t) \tag{3}$$

where $f(\theta, t)$ is the MMF of the air gap and $\lambda(\theta, t)$ is the air gap permanence. $f(\theta, t)$ can be expressed as (4).

$$\begin{aligned} f(\theta,t)=&F_p\cos(P\theta-2\pi f_s t-\phi_p)\\ &+\sum_v F_v\cos(v\theta-2\pi f_s t-\phi_v)\\ &+\sum_\mu F_\mu\cos(\mu\theta-2\pi f_\mu t-\phi_\mu) \end{aligned} \tag{4}$$

where P is the number of pole pairs and f_s is the fundamental frequency of the power supply. The first

term in (4) is the fundamental component of the air gap MMF, the second and third terms are the MMF harmonics produced by the stator and rotor currents, respectively. In an induction motor with the number of stator slots Z_s and the number of rotor slots Z_r, Eqs. (5)–(7) defined.

$$v = q_s Z_s + p \qquad q_s = \pm 1, \pm 2, \ldots \tag{5}$$

$$\mu = q_r Z_r + p \qquad q_r = \pm 1, \pm 2, \ldots \tag{6}$$

$$f_\mu = f_s \left[1 + \frac{q_r Z_r}{p} (1 - s_1) \right] \tag{7}$$

In (7), s_1 is the rotor slip at the fundamental frequency.

The air gap permanence $\lambda(\theta, t)$ is affected by the width of the rotor and stator slots and can be expressed as (8).

$$\lambda(\theta,t) \approx \Lambda_0 + \sum_{k_s = \pm 1, \pm 2, \ldots} \Lambda_{k_s} \cos\left(k_s Z_s \theta\right) + \sum_{k_r = \pm 1, \pm 2, \ldots} \Lambda_{k_r} \cos\left(k_r Z_r \left[\theta - \frac{2\pi f_s}{p} (1 - s_1) t \right] \right) \tag{8}$$

In (8), Λ_0 is the average air gap permanence, Λ_{ks} and Λ_{kr} are the amplitudes of the permanence harmonics of the width of stator and rotor slots, respectively.

By replacing (4) and (8) in (3) and regardless of some of the components, the radial field of the air gap $b_r(\theta, t)$ can be rewritten as (9).

$$\begin{aligned} b_r(\theta,t) \approx\ & F_p \Lambda_0 \cos\left(P\theta - 2\pi f_s t - \phi_p\right) \\ & + \sum_v F_v \Lambda_0 \cos\left(v\theta - 2\pi f_s t - \phi_v\right) \\ & + \sum_{k_s = \pm 1, \pm 2, \ldots} 0.5 F_p \Lambda_{k_s} \cos\left[\left(k_s Z_s + p\right)\theta - 2\pi f_s t - \phi_p \right] \\ & + \sum_\mu F_\mu \Lambda_0 \cos\left(\mu\theta - 2\pi f_\mu t - \phi_\mu\right) \\ & + \sum_{k_r = \pm 1, \pm 2, \ldots} 0.5 F_p \Lambda_{k_r} \cos\left(\left(k_r Z_r + p\right)\left[\theta - 2\pi f_{k_r} t - \phi_p \right] \right) \end{aligned} \tag{9}$$

In (9), f_{kr} is defined as (10).

$$f_{k_r} = f_s \left[1 + \frac{k_r Z_r}{p} (1 - s_1) \right] \tag{10}$$

According to (9), the radial field of the air gap consists of the following: The first expression represents the air gap field at the fundamental frequency $b_{r_p}(\theta,t)$, the second expression is the harmonics of the air gap field caused by the MMF harmonics of the stator slot $b_{r_{sf}}(\theta,t)$, the third term is the harmonic of the field of distances created by the permanence harmonics of the stator slot $b_{r_{s\lambda}}(\theta,t)$, the fourth expression is the harmonics of the air gap field generated by the MMF of the slot $b_{rrf}(\theta,t)$ and the fifth term is the harmonics of the air gap field caused by the permanence harmonics of the rotor are $b_{rr_\lambda}(\theta,t)$. The components $b_{r_{sf}}(\theta,t)$ and $b_{r_{s\lambda}}(\theta,t)$ when $k_s = q_s$ have the same spatial order v and f_s. In addition $b_{r_{sf}}(\theta,t)$ and $b_{r_{s\lambda}}(\theta,t)$ can be combined with each other and, as the air gap field harmonics of the stator slots $b_{r_s}(\theta,t)$ by (11) is expressed.

$$b_{r_s}(\theta,t) = \sum_{k_{s=\pm 1, \pm 2, \ldots}} B_{rs_{k_s}} \cos\left[\left(k_s Z_s + p\right)\theta - 2\pi f_s t \right] \tag{11}$$

Therefore, $b_r(\theta, t)$ can be rewritten as (12).

$$b_r(\theta,t) = b_{r_p}(\theta,t) + b_{r_{sf}}(\theta,t) + b_{rrf}(\theta,t) + b_{rr_\lambda}(\theta,t) \tag{12}$$

Finally, the radial Maxwell pressure P_m can be expressed as (13) [34].

$$P_m(\theta,t) \approx \frac{b_{r_s}(\theta,t)\left[b_{rrf}(\theta,t) + b_{rr_\lambda}(\theta,t) \right]}{2\mu_0} \tag{13}$$

3 Common Single-Phase Induction Motors

3.1 The First Type of Motor

This is the America Westinghouse-designed motor with a temporary starting winding. At the starting time, both main and auxiliary windings are energized, but the auxiliary winding is removed from the circuit by the centrifugal switch when the motor speed reaches 60-80% of the synchronous speed. Therefore, in the motor,s steady-state operation, only a single winding (high or low speeds) remains in the circuit. In this structure of the motor, due to the temporary start winding of it, the start is made of 4 poles. Therefore, at the start, it first starts at high speed (4 poles) and switches to low speed (6 poles) when the speed reaches 60- 80% of the synchronous speed. This motor has 3 layers of windings (high, low, and auxiliary). The design of the stator structure of this motor, as shown in Fig. 1, has slots with different geometry. So in their winding, the selection of the start slot for the winding is important. The windings of this motor are concentricity and full pitch. The widespread designs of this motor's windings are shown in Figs. 2 and 3.

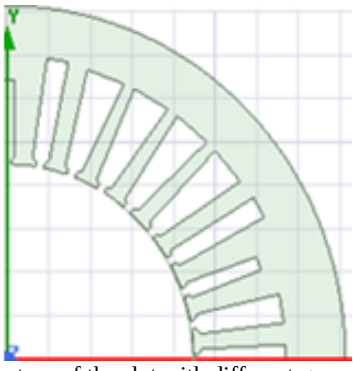

Fig. 1 Structure of the slot with different geometry of the American design motor.

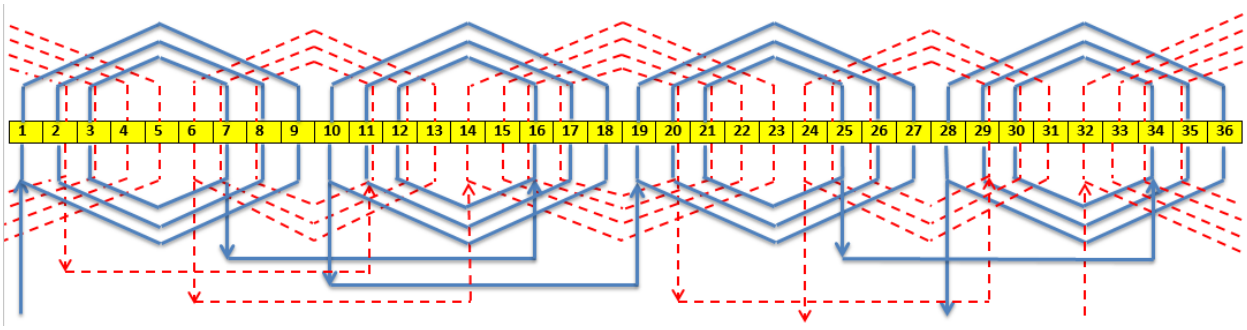

Fig. 2 The widespread design of High-speed (solid line) and auxiliary windings (dashed line) of the first type motor.

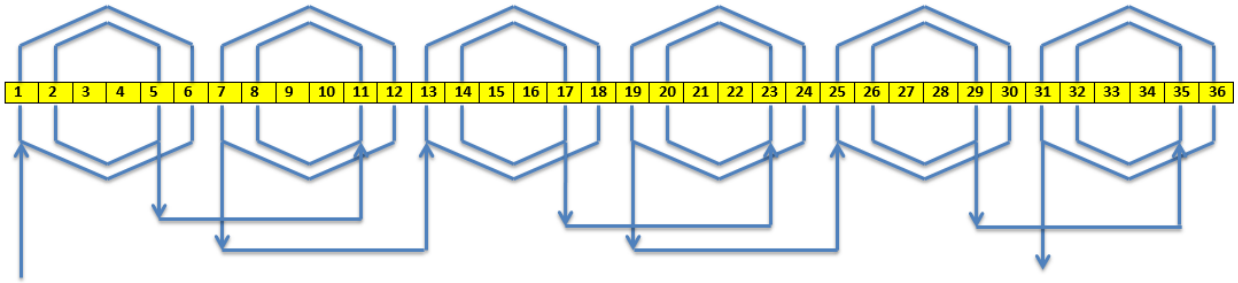

Fig. 3 The widespread design of low-speed of the first type of motor.

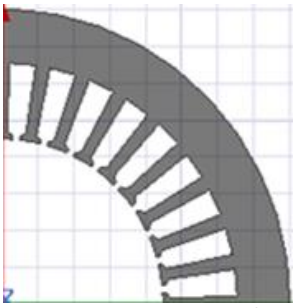

Fig. 4 The slot structure with the same geometry of the stator designed by Italy.

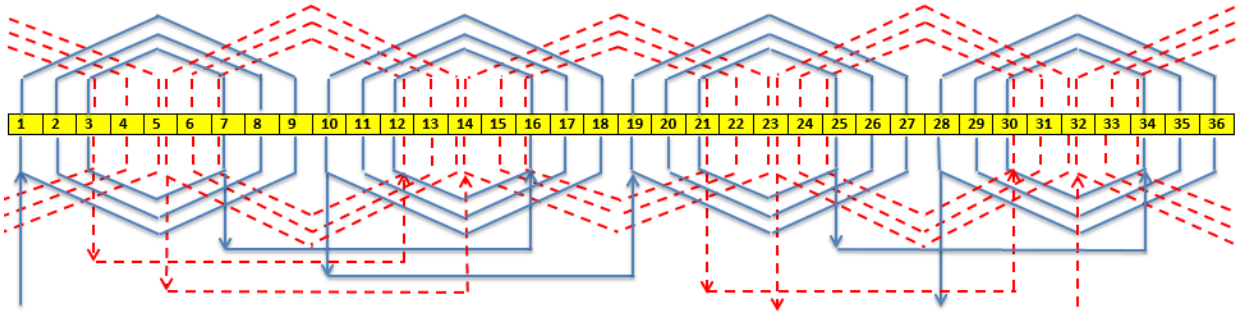

Fig. 5 The widespread design of high-speed (solid line) and auxiliary windings (dashed line) of the second type motor.

3.2 The Second Type Motor

This motor is Italy's design. As shown in Fig. 4, all its stator slots are quite similar to each other. Compared to the first motor type, this one has a larger core length but an equal stator diameter. In this motor, the centrifugal switch is not used for switching high and low speeds. Therefore, each of the high and low-speed windings has a separate auxiliary winding and the auxiliary windings remain in the circuits by constant capacitors. This motor has 4 layer windings. The winding of this motor is a concentricity and full-pitch winding. The widespread designs of this motor's windings are shown in Figs. 5 and 6.

4 Introductions the New Winding Designs to Reduce Magnetic Pressure

Given that one of the most important parameters affecting noise and magnetic pressure is the distribution of machine windings, in this paper two new single-phase induction motor winding designs will be

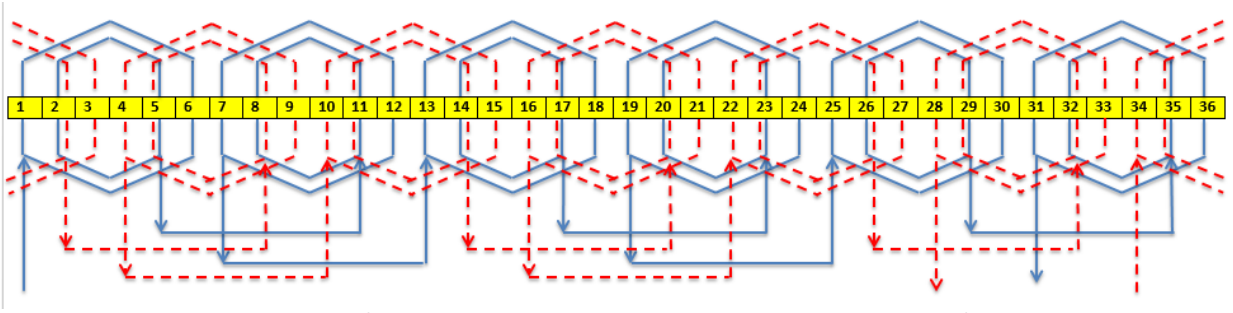

Fig. 6 The widespread design of low-speed (solid line) and auxiliary windings (dashed line) of the second type motor.

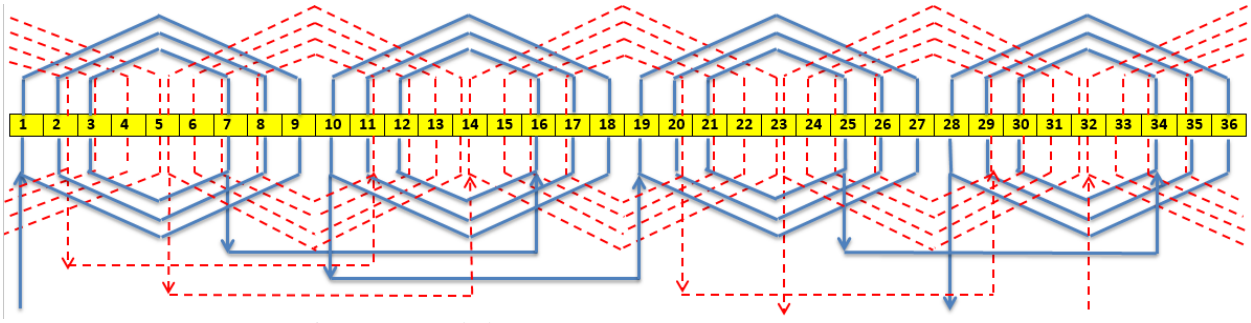

Fig. 7 The widespread design of the proposed design 1: high-speed (solid line) and its auxiliary windings (dashed line) – 4 poles.

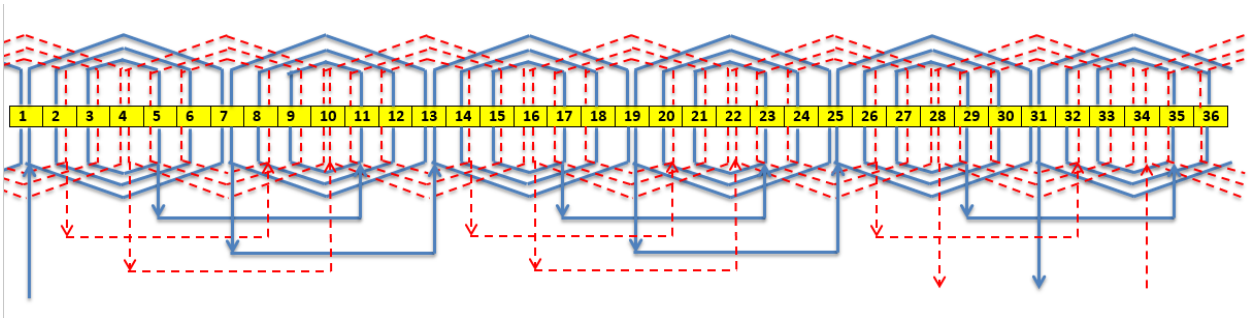

Fig. 8 The widespread design of the proposed design 1: high-speed (solid line) and its auxiliary windings (dashed line) – 6 poles.

presented to reduce the magnetic pressure. Continuing with the introduction of these windings, we will compare the performance of the motor in the presence of conventional and proposed windings.

4.1 Proposed Winding; Type1

Proposed winding 1 is concentricity and full pitch. It is similar to the American and Italian design windings, but in this design, it has been tried to reinforce the center of the poles by changing the pitch of coils and increasing the number of conductors at the center of the poles. The closer we get to the edge of the poles, the effect gets weaker. As a result, its winding function becomes closer to its sinusoidal distribution and leading to an increase in the amplitude of the fundamental component and a decrease in the amplitude of the other harmonic components, thereby reducing THD. The stator has the same slot structure as the Italian design. All windings are concentricity and full pitch. This motor includes 4 layers of high-speed and auxiliary windings and a low-speed and auxiliary windings. Auxiliary windings remain permanently in the circuit. The space slot factor in this design is 0.39. The widespread designs of the windings in its high speed and auxiliary, as well as low speed and its auxiliary windings, are shown in Figs. 7 and 8.

4.2 Proposed Winding; Type2

In this winding design, the coils are stacked together with the same pitch. That's why they are called lap, chain, or so-called overhead winding. The stator slots have the same geometry as the Italian design. The winding has four layers. Start windings remain in the circuit. The pitch of the main and auxiliary windings at high speeds is 7 and the pitch of the main and auxiliary windings at a low speed is 5. The main advantages of this design to concentricity windings (previous designs) are the following: reduction of time in the preparation of winding molding, wrapping and welding of coils, reducing the average length of coils, reduces copper consumption, cost-effectiveness, the possibility of parallel connection of each group of coils to each other and also the connection of the individual coils. Its winding function is different from concentric winding

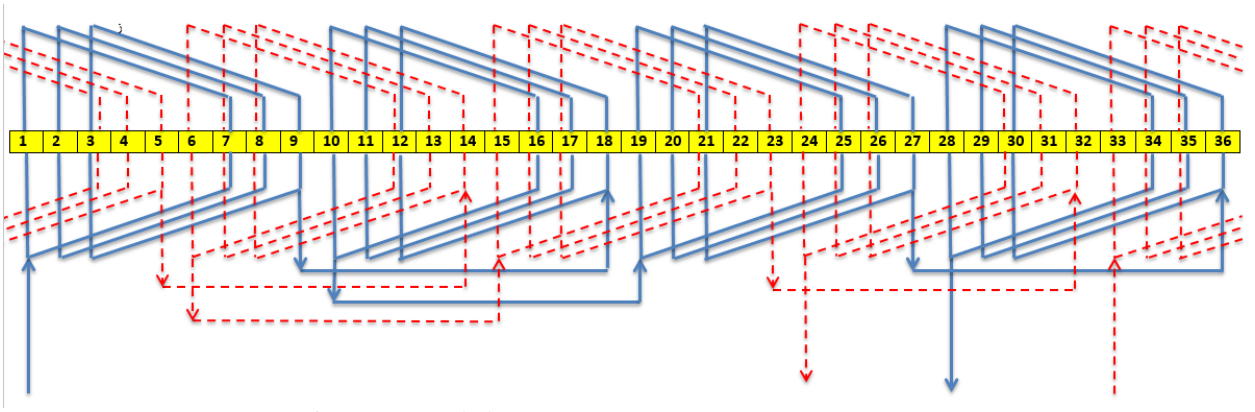

Fig. 9 The widespread design of the proposed design 2: high-speed (solid line) and its auxiliary windings (dashed line) – 4 poles.

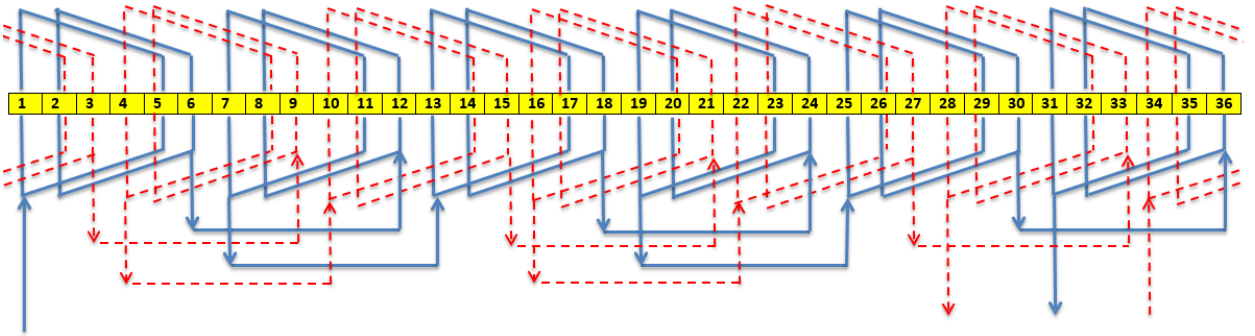

Fig. 10 The widespread design of the proposed design 2: high-speed (solid line) and its auxiliary windings (dashed line) – 6 poles.

and has fewer harmonic components. By applying this winding type to the stator and comparing its results with American and Italian designs, more favorable results were obtained. The space slot factor in this design is 0.33. The widespread designs of the high-speed and its auxiliary windings and the low-speed and its auxiliary windings are shown in Figs. 9 and 10, respectively.

5 Analyze and Comparison of Different Windings

In order to compare the different designs of the windings, the American and Italian designs, along with the two proposed designs of this paper, are evaluated in two analytical and numerical methods. An analytical comparison will be made by the relationships in Section 2 and numerical comparison with Maxwell software. The electrical characteristics and the mechanical parameters of the single-phase induction motors are shown in Tables 2 and 3, respectively.

5.1 Magnetic Field Distribution

The variations in the magnetic flux density in the 4 and 6 poles states are shown in Figs. 11 and 12, respectively. The fast Fourier transform (FFT) analyses of these signals are shown in Figs. 13 and 14, respectively.

Winding distribution of the American and Italian designs, despite their differences, is very similar to each other. The winding function of both of them has only differences in its step values. Therefore, it can be expected that both motors have almost identical spatial

Table1 The electrical characteristics of the single-phase induction motors.

	Parameters	Values			
		American design	Italian design	Proposed design 1	Proposed design 2
High speed	Output power [hp]	0.75	0.75	0.75	0.75
	Frequency [Hz]	50	50	50	50
	Voltage [V]	220	220	220	220
	Speed [RPM]	1500	1500	1500	1500
	Start capacitor [µf]	455	-	430	430
	Run capacitor [µf]	70	16	16	16
Low speed	Output power [hp]	0.25	0.25	0.25	0.25
	Frequency [Hz]	50	50	50	50
	Voltage [V]	220	220	220	220
	Speed [RPM]	1000	1000	1000	1000
	Start capacitor [µf]	455	-	430	430
	Run capacitor [µf]	70	9	12	12

Table2 The mechanical parameters of the single-phase induction motors.

Parameters		Values	
		American design	Italian and Proposed designs
Stator	Outer diameter [mm]	161.3	160.6
	Inner diameter [mm]	89.7	89.8
	Length [mm]	55	66
	Number of slots	36	36
Air gap [mm]		0.46	0.45
Rotor	Outer diameter [mm]	88.8	88.9
	Number of slots [mm]	49	49

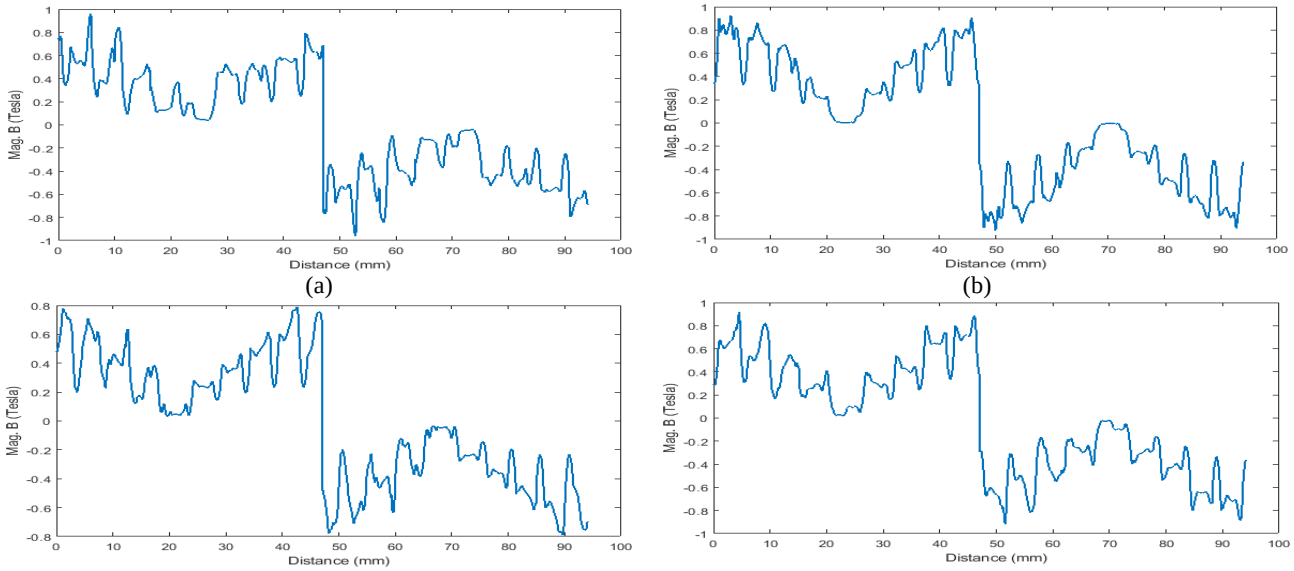

Fig. 11 Variation of flux density – 4 poles; a) American design, b) Italian design, c) Proposed design 1, and d) Proposed design 2.

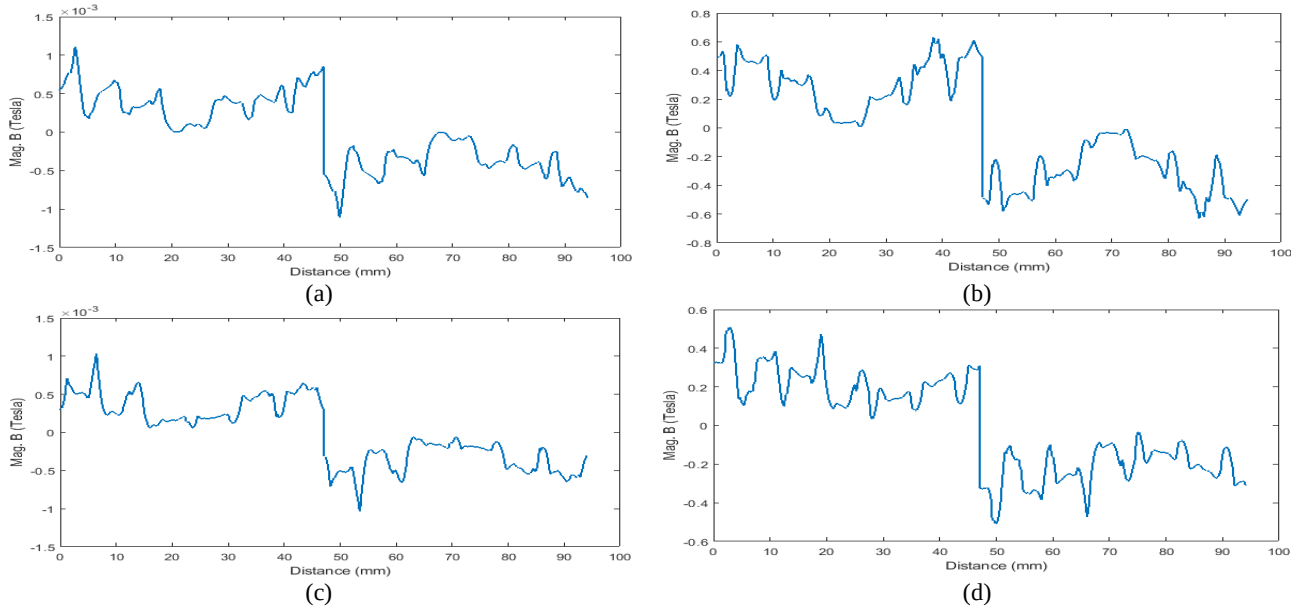

Fig. 12 Variation of flux density – 6 poles; a) American design, b) Italian design, c) Proposed design 1, and d) Proposed design 2.

harmonics. But the distribution of the winding and the resulting winding function is different in the proposed designs with the two previous types. In these designs, in both high and low speeds, two windings are simultaneously in the circuit. Due to the difference in the capacitors that have been seized with each of these windings, a phase difference arises between their fields. The performance of these two fields causes the motor to perform more efficiently. It is also worth noting that the amount of copper used in American, Italian, proposed 1 and proposed 2 designs is 324, 347, 270 and 235 grams, respectively. As it is known, the amount of copper used in the proposed projects has decreased compared with existing motors.

5.2 Comparison of Motor Speed Dynamic Performance

Fig. 15 shows the speed-time curves of modeled motors at high-speed (4-poles) under a load of 2N.m overtime of 130ms. Accordingly, the settling time (t_s) in all curves is approximately equal, the rise time (t_r) in the two American design models and the proposed design 2 is less than 20ms, in the proposed design 2 is about 30ms, and in the Italian design is about 60ms. The overshoot (MP%) in the two American models and proposed design 2 is about 30% and in the Italian models and proposed design 1 is about 20%. Also, Fig. 16 shows the speed-time curves of various types of simulated motors at low speed (6-poles) under a load of 1N.m over a 130ms time. As shown, settling time (t_s) is

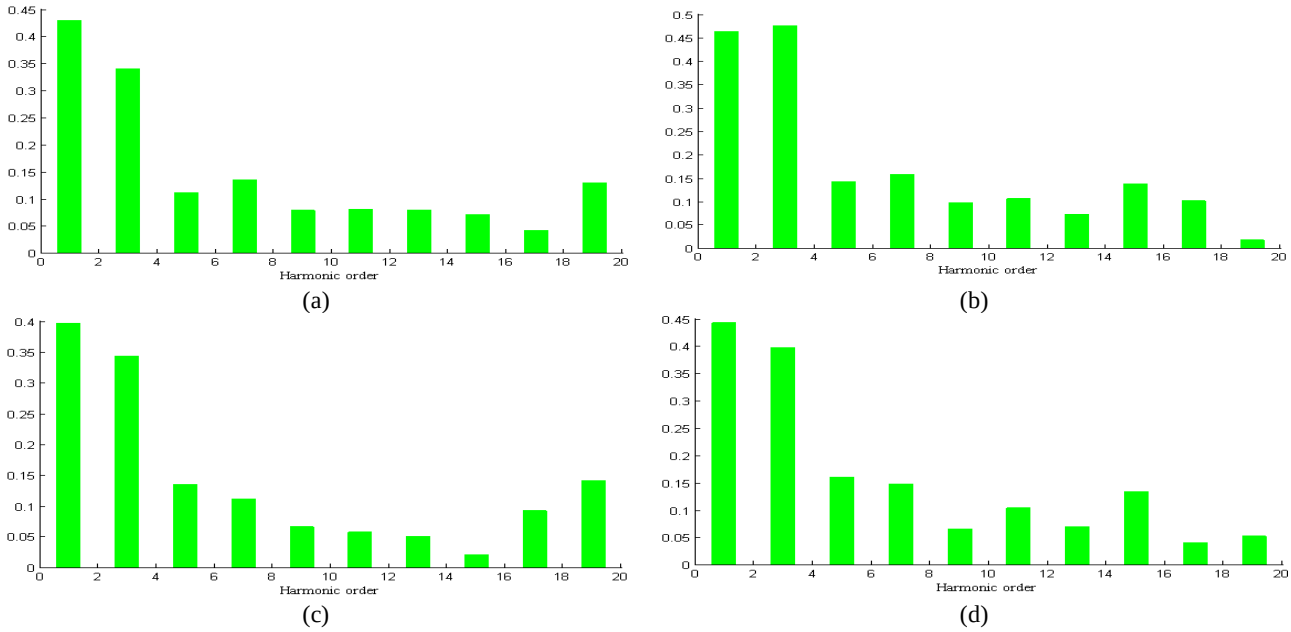

Fig. 13 Fourier analysis of flux density variations- 4 poles; a) American design, b) Italian design, c) Proposed design 1, and d) Proposed design 2.

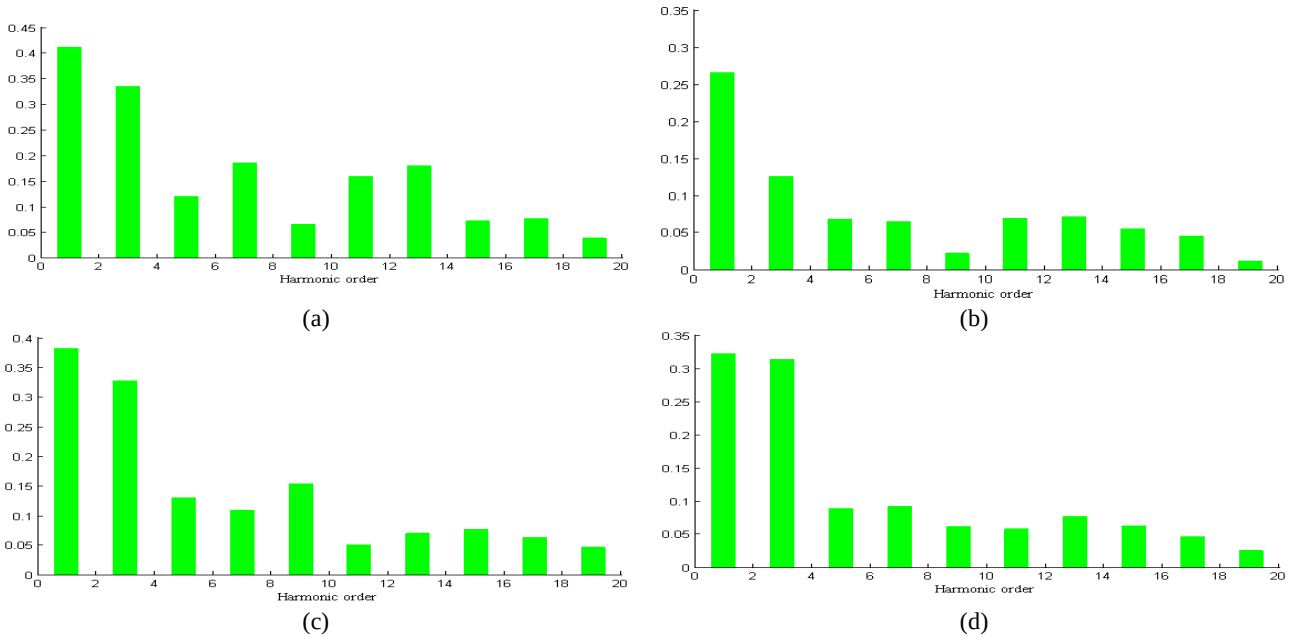

Fig. 14 Fourier analysis of flux density variations- 6 poles; a) American design, b) Italian design, c) Proposed design 1, and d) Proposed design 2.

in the two American models and proposed design 1 is about 50ms and in the two Italian and proposed design 2 are about 90ms. The rise time (t_r) is equal to almost all models. Overshoot (MP%) in proposed design 2 is about 30% and in other designs is about 20%. The curves of main winding current in the scale of time of the various types of simulated motors at high speed (4 poles) under a load of 2N.m and at a low speed (6 poles) under a load of 1N.m overtime of 130ms, are shown in Figs. 17 and 18, respectively.

Torque-time curves of different types of simulated motors at high speed (4 poles) under a load of 2N.m and at a low speed (6 poles) under a load of 1N.m overtime of 130ms are shown in Figs. 19 and 20, respectively. The curves of the electromagnetic force for various types of motors (calculated by Maxwell software) at high speed (4 poles) under a load of 2N.m and at low speed (6 poles) under a load of 1N.m overtime of 130ms are shown in Figs. 21 and 22, respectively.

The results of the simulation of a variety of simulated models by Maxwell software at two speeds are summarized in Table 3. These results include winding

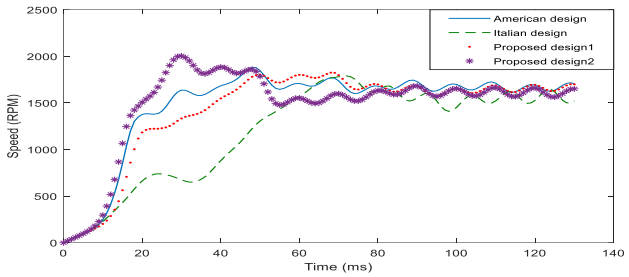

Fig. 15 Speed-time curves – 4 poles.

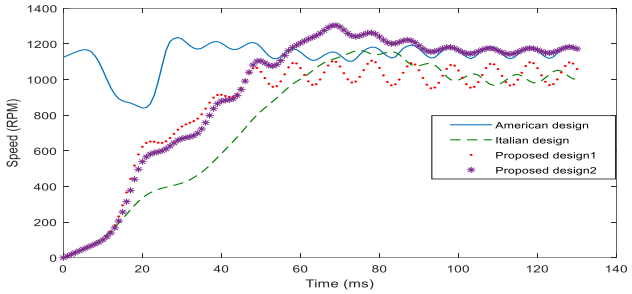

Fig. 16 Speed-time curves – 6 poles.

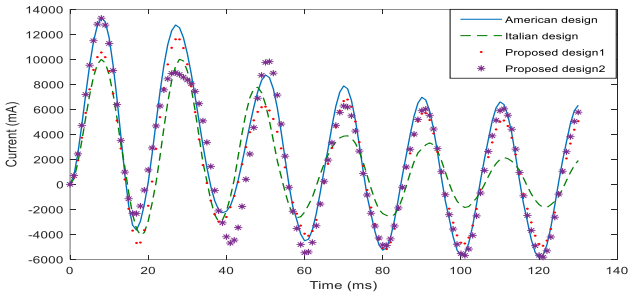

Fig. 17 Current-time curves of the main windings – 4 poles.

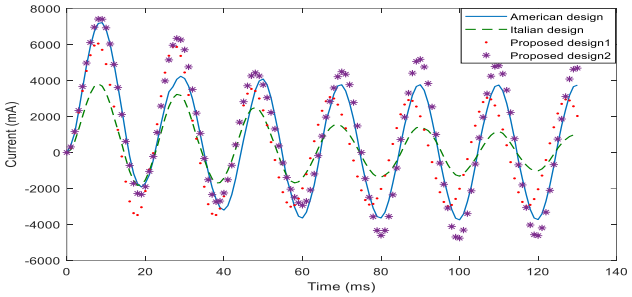

Fig. 18 Current-time curves of the main windings – 6 poles.

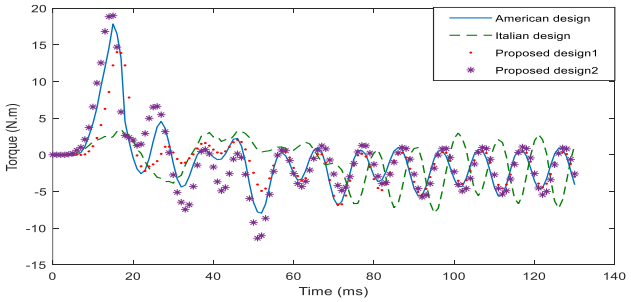

Fig. 19 Torque-time curves – 4 poles.

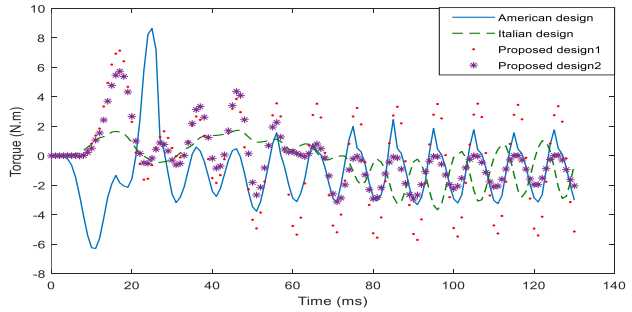

Fig. 20 Torque-time curves – 6 poles.

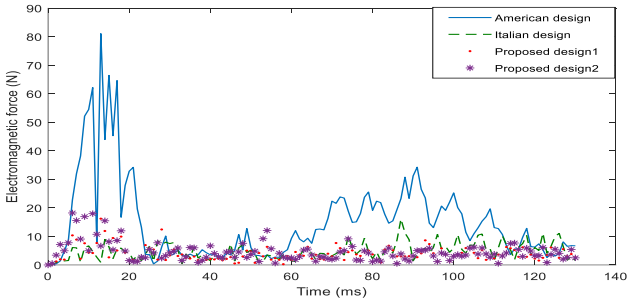

Fig. 21 Electromagnetic force-time curves – 4 poles.

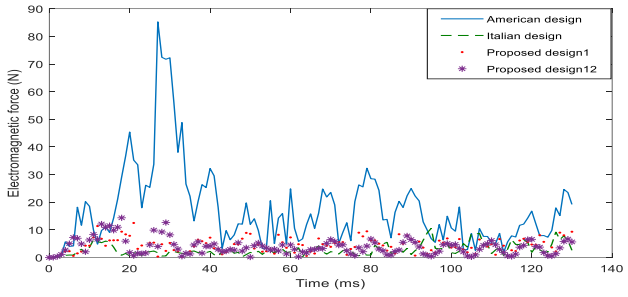

Fig. 22 Electromagnetic force-time curves – 6 poles.

Table 3 The comparison of the parameters of 4 different motors.

Quantity \ Motor		American design		Italian design		Proposed design 1		Proposed design 2	
		High speed	Low speed	High speed	Low speed	High speed	Low speed	High speed	Low Speed
Current [A]	Main	7	3.75	2.5	1	5	3	6	4.8
	Auxiliary	17	-	4.2	2	2	3.7	4	1.5
Resistance [Ω]	Main	3.1	11.2	4.5	20.6	4.5	15	3.9	7.8
	Auxiliary	7.5	-	14.2	67.4	6.9	26	5	12
Torque ripple [N.m]		3.25	2.5	5.1	2	2.25	4.4	2.5	1
The calculated average of Maxwell radial force magnitude by the numerical method [N]		14.78	17.26	4.85	2.87	3.92	4.45	4.58	3.89
the calculated average of Maxwell radial force magnitude by analytical method [N]		17.66	17.81	13.95	6.5	9.61	13.11	12.06	3.25
The THD of flux density [%]		83	87	73	45	69	68	71	65
Total copper consumed [g]		324		347		270		235	

current and resistance, torque ripple, average Maxwell radial force and air gap THD flux density, which is derived from the curves mentioned. In addition, the average amount of radial force is theoretically calculated through relationships and can be seen in Table 3.

6 Conclusion

The purpose of this paper is to present a new winding distribution design to reduce electromagnetic noise in single-phase induction motors. In this regard, two proposed designs for the distribution of the winding are provided and the behavior of the electromagnetic forces in them is compared with existing winding designs. The results show that the proposed designs, reduce the air gap THD flux density, and consequently reduce the average value of the Maxwell radial forces applied to the stator and rotor cores. Also, ripple torque has dropped in proposed designs in contrast to existing designs except at the low speed of the proposed proposal 1. In spite of the use of more windings, the amount of copper consumed in the proposed designs has decreased.

References

[1] P. S. Bimbhara, *General theory of electrical machines*. Khana Publishers Delhi, 1983.

[2] P. Vijayraghavan and R. Krishnan, "Noise in electric machines: A review," *IEEE Transactions on Industry Applications*, Vol. 35, No. 5, pp. 1007–1013, 1999.

[3] R. E. Araújo, Ed., *Induction motors: Modelling and control*. InTech Open, 2012.

[4] R. S. Curiac and S. Singhal. "Magnetic noise in induction motors," in *Proceedings of Noisecon/ASME NCAD*, 2008.

[5] R. S. Girgis and S. P. Vermas, "Method for accurate determination of resonant frequencies and vibration behavior of stators of electrical machines," in *IEE Proceedings B* (*Electric Power Applications*), Vol. 128, No. 1, pp. 1–11, 1981.

[6] S. Watanabe, S. Kenjo, K. Ide, F. Sato, and M. Yamamoto, "Natural frequencies and vibration behavior of motor stator," in *IEEE Transactions on Power Apparatus and Systems*, Vol. 102, No. 4, Apr. 1983.

[7] J. L. Besnerais, V. Lanfranchi, M. Hecquet, P. Brochet, and G. Friedrich, "Acoustic noise of electromagnetic origin in a fractional-slot induction machine," *COMPEL: The International Journal for* Computation *and Mathematics in Electrical and Electronic Engineering*, Vol. 27, No. 5, pp. 1033–1052, 2008,

[8] J. L. Besnerais, V. Lanfranchi, M. Hecquet, G. Lemaire, E. Augis, and P. Brochet, "Characterization and reduction of magnetic noise due to saturation in induction machines," *IEEE Transaction on Magnetics*, Vol. 45, No. 4, pp. 2003–2008, Apr. 2009.

[9] B. Cassoret, R. Corton, D. Roger, and J. Brudny, "Magnetic noise reduction of induction machines," *IEEE Transactions on Power Electronics*, Vol. 18, No. 2, pp. 570–579, 2003.

[10] J. Le Besnerais, V. Lanfranchi, M. Hecquet, and P. Brochet, "Optimal slot numbers for magnetic noise reduction in variable-speed induction motors," *IEEE Transactions on Magnetics*, Vol. 45, No. 8, pp. 3131–3136, Aug. 2009.

[11] I. Peter, G. Scutaru, and R. Ionescu, "The magnetic noise of three-phase and single-phase induction motors with squirrel cage rotors," *IEEE EUROCON 2009*, St. Petersburg, Russia, 2009.

[12] T. G. D. Hilgert, L. Vandevelde, and J. A. A. Melkebeek, "Numerical analysis of the contribution of magnetic forces and magnetostriction to the vibrations in induction machines," *IET Science, Measurement & Technology*, Vol. 1, No. 1, pp. 21–24, 2007.

[13] P. Pellerey, V. Lanfranchi, and G. Friedrich, "Coupled numerical simulation between electromagnetic and structural models. influence of the supply harmonics for synchronous machine vibrations", *IEEE Transactions on Magnetics*, Vol. 48, No. 2, pp. 983–986, Feb. 2012.

[14] C. Schlensok, B. Schmülling, M. Van Der Giet, and K. Hameyer, "Electromagnetically excited audible noise – Evaluation and optimization of electrical machines by numerical simulation," *COMPEL: The International Journal for Computation and Mathematics in Electrical and Electronic Engineering*, Vol. 26, No. 3, pp. 727–742, 2007.

[15] T. Kobayashi, F. Tajima, M. Ito, and S. Shibukawa, "Effects of slot combination on acoustic noise from induction motors," *IEEE Transactions on Magnetics*, Vol. 33, No. 2, pp. 2101–2104, 1997.

[16] J. L. BESNERAIS, "Vibro-acoustic analysis of radial and tangential air gap magnetic forces in permanent magnet synchronous machines," *IEEE Transactions on Magnetics*, Vol. 51, No. 6, Jun. 2015.

[17] D. Mori and T. Ishikawa, "Force and vibration analysis of induction motors," *IEEE Transactions on Magnetics*, Vol. 41, No. 5, pp. 1948–1951, Jun. 2005.

[18] J. Le Besnerais, "Reduction of magnetic noise in PWM-supplied induction machines – low-noise design rules and multi-objective optimization", *Ph.D. Dissertation*, 2008

[19] K. S. Huang, Z. G Liu, H. Li, J. Yang, D. R. Turner, L. Jiang, and Q. H. Wu, "Reduction of electromagnetic noise in three-phase induction motors," in *International Conference on Power System Technology*, Kunming, China, Oct. 2002.

[20] D. J. Kim, J. W. Jung, J. Hong, K. Kim, and C. J. Park, "A study on the design process of noise reduction in induction motors", *Transactions on Magnetics*, Vol. 48, No. 11, pp. 4638–4941, Nov. 2012.

[21] G. Y. Zhou and J. X. Shen, "Rotor notching for electromagnetic noise reduction of induction motors," *IEEE Transactions on Industry Applications*, Vol. 53, No. 4, pp. 3361–3370, 2017.

[22] A. Negoita and R. M. Ionescu, "Influence of rotor static eccentricity on the noise level of a squirrel cage induction motor," in *10th International Conference on Environment and Electrical Engineering*, Rome, Italy, May 2011.

[23] H. Ebrahimi, Y. Gao, H. Dozono, and K. Muramatsu, "Effects of stress and magnetostriction on loss and vibration characteristics of motor," *IEEE Transactions on Magnetics*, Vol. 52, No. 3, Mar. 2016.

[24] M. Kuroishi and A. Saito, "Effects of magnetostriction on electromagnetic motor vibration at sideband frequencies," *IEEE Transactions on Magnetics*, Vol. 54, No. 2, Feb. 2018.

[25] A. Belahcen, "Vibrations of rotating electrical machines due to magneto mechanical coupling and magnetostriction," *IEEE Transactions on Magnetics*, Vol. 42, No. 4, pp. 971–974, Apr. 2006.

[26] M. Tsypkin, "The origin of the electromagnetic vibration of induction motors operating in modern industry: Practical experiance – Analysis and diagnostics," in *Petroleum and Chemical Industry Technical Conference (PCIC)*, Philadelphia, PA, USA, Sep. 2016.

[27] T. Jung, C. H. Yun, H. R. Cha, M. G. Chae, and H. M. Kim, "Improved design for driving characteristics in single phase induction motor with concentrated winding," *IEEE Power Electronics Specialists Conference*, Orlando, FL, USA, Jun. 2007.

[28] P. La Delfa, M. Hecquet, and F. Gillon, "Radial pressure analysis in PMSM responsible for electromagnetic noise," in *11th France-Japan & 9th Europe-Asia Congress on Mechatronics* (*MECATRONICS*), Compiegne, France, Jun. 2016.

[29] S. Ayari, M. Besbes, M. Lecrivain, and M. Gabsi, "Effects of the airgap eccentricity on the SRM vibrations," *IEEE International Electric Machines and Drives Conference (IEMDC'99)*, Seattle, USA, May 1999.

[30] S. M. Hosseini, "Performance improvement of capacitor-run single-phase induction motors by non-orthogonal armature windings," *International Symposium on Power Electronics, Electrical Drives, Automation and Motion* (*SPEEDAM*), Anacapri, Italy, Jun. 2016.

[31] A. K. Sedigh and M. T. Hagh, "Elimination of instantaneous backward mmf in single phase induction motors," in *5th IEEE GCC Conference & Exhibition*, Kuwait City, Kuwait, Mar. 2009.

[32] H. Zhong, X. Wang, X. Leng, and D. Wang, "A new type single-phase induction motor with negative sequence compensatory winding," in *2nd IEEE Conference on Industrial Electronics and Applications*, Harbin, China, May 2007.

[33] J. F. Gieras, C. Wang, and J. C. Lai, *Noise of polyphase electric motors*. Boca Raton, FL: CRC Press, 2005.

[34] G. Y. Zhou and J. X. Shen, "Rotor notching for electromagnetic noise reduction of induction motors," *IEEE Transactions on Industry Applications*, Vol. 53, No. 4, pp. 3361–3370, 2017.

H. Shadfar received the M.Sc. degree from Semnan University, Semnan, Iran. He is currently working toward the Ph.D. degree in Faculty of Electrical and Computer Engineering, Semnan University, Semnan, Iran. His major research interests include designing and modeling of electric machines.

H. R. Izadfar is currently an Assistance Professor in Electrical and Computer Engineering Department of Semnan University. His main research interests are design and analytical and numerical analysis of electric machines and drives.